ZIBELINE INTERNATIONAL™ PUBLISHING

Pakistan Journal of Geology (PJG)

DOI: http://doi.org/10.26480/pjg.01.2026.01.11

ISSN: 2521-2915 (Print)
ISSN: 2521-2923 (Online)
CODEN: PJGABN

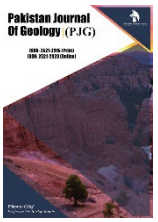

RESEARCH ARTICLE

GEOCHEMICAL INSIGHTS INTO COASTAL PLAIN SANDS: SAPELE BYPASS BENIN REGION NIGERIA

Martins Ilevbare*

Department of Geology, College of Science, Afe Babalola University Ado - Ekiti, Nigeria
Corresponding Author Email: martins.ilevbare@abuad.edu.ng

ARTICLE DETAILS

Article History:

Received 20 January 2026
Revised 25 January 2026
Accepted 19 February 2026
Available online 28 February 2026

ABSTRACT

The coastal plain sand Coastal sand, Osbedoluogbeyi and Idogbo comunities along Sapele bypass in Benin Region, Nigeria were analysed for Geochemical Characterisation. Twenty-one (21) samples were collected in which 7 samples were analysed for major oxides, 7 for trace elements, and 7 rare earth elements. The samples were analyzed using X-Ray fluorescence (XRF) and inductively coupled plasma mass spectrometre (ICP-MS). The provenance from the major oxides inferred that the samples were from felsic igneous source rocks (Al_2O_3/TiO_2: ~29.90). The source area weathering of the sand shows that the sediment has undergone substantial to intense chemical weathering (CIA ~61.40; CIW ~83.00; MIA ~41.00; PIA ~77.07). The maturity of the sand is mature (SiO_2/Al_2O_3 ~6.22). The trace elements geochemistry also authenticates the provenance as felsic source. The outcomes from the Correlation and Chi-square of the metallic oxides indicates an enrichment of silica and depletion of other oxides as well as indicates a common source. The coastal sand is most likely to be a reservoir rock for hydrocarbon potential, if it is a petroleum system with source and trap rather than a source rock.

KEYWORDS

Coastal Sands, Chemical weathering, Provenance, Source Rock, Petroleum system

1. INTRODUCTION

The physical characteristics of the Benin Region which are relevant for the purpose of this investigation are hereby discussed in terms of those factors which identified as the environment of weathering, (Ajadi et al., 2020).

They include the geological foundation and rock types, types and density of plant cover, availability of readily weather able rocks, and tropical humid climate with seasonality of rainfall or alternating wet and dry seasons and topography amongst others, (Haque et al., 2019; Ilevbare and Omoruyi, 2020).

According to the study, the geology and geomorphologic processes and landforms of the Benin Region have their interplay/interconnections with weathering (Akujieze, 2004). In a broad term, the geomorphology includes aspects of the geology and relief while the hydrology embraces aspects of the drainage and water resources. These are discussed below under the following headings: Geology, Physiography (Relief) and Geomorphology, Geomorphic Processes, Weathering, Drainage Processes, Landforms, Surface Water Hydrology and Water Resources. These aspects have not been fully documented by research workers in this region.

The oil and gas industry in Nigeria is facing a significant challenge of finding answers to whether future hydrocarbon supply can keep pace with the increasing demand at a competitive price. Considering our non-renewable oil reserves, it's certain that continuous exploitation of the Niger-Delta Basin for hydrocarbon and its associated products, in no time might plunge the country into an economic crisis.

This research focuses on whether a thorough study into the Geochemistry of the Benin region sand can help to provide an insight into the likely reservoir maturity and provenance of the coastal plain sediments, therefore fostering exploration and exploitation of the sediments.

1.1 Regional Geology of Benin Region Sediments

The Benin Region (Figure 1) is underlain by sedimentary formation of the South Sedimentary Basin. The geology is generally marked by top reddish earth, composed of ferruginized or literalized clay sand. First used the term Benin sand to describe the reddish earth underlain by sands, sandy clays and ferruginized sandstone that mark the Paleo-Coastal Environment of Paleocene-Pleistocene Age (Ikhile, 2016). These sediments spread across the southern fringes of the Anambra Basin and marking the upper fancies off-flaps of the Niger Delta. As, used the name Coastal plain sands to describe the formation of red earth underlain by sands and clays that mark an ancient coastal plain environment now exposed in Calabar, Owerri, Onitsha and the Benin Region with the age Oligocene-Pleistocene (Ikhile, 2016).

Ighodaro *et al.*, (2018) reinstated the name Benin formation to identify the reddish-brown-yellow generally white sands often with clayey and pebbly horizons with type-locality around Benin. This is also referenced at Calabar and other parts of South Eastern Nigeria. The formation was further established by well logging of Etete 1, well drilled on-shore east of River Niger by Shell Nigeria. Petroleum Development Company (SPDC) and described by (Ajakaiye and Oti, 2016). The formation is about 1830 m thick at the seashore but thins landwards. The sedimentary suits of the Benin Formation dip 2° - 8° south. Geologically, the Benin Region comprises of; Benin formation, Alluvium, Drift/top soil and Azagba-Ogwashi (Asuba-Ogwashi) formation.

1.2 Benin Formation

It is assigned to the Oligocene-Pleistocene period in the continent of Africa and to the Oligocene-Pleistocene recent at the sub-oceanic (Akinyemi et al., 2015). The formation is characterized by top reddish to reddish brown lateritic massive fairly indurate clay and sand. This is often marked with

Quick Response Code	Access this article online	
	Website: www.pakjgeology.com	**DOI:** 10.26480/pjg.01.2026.01.11

Cite the Article: Martins Ilevbare (2026). Geochemical Insights into Coastal Plain Sands: Sapele Bypass Benin Region Nigeria. *Pakistan Journal of Geology, 10(1): 01-11.*

reticulate mud cracks. This cap the underlying more friable pinkish-yellowish white often gravelly-pebble sands clayey soils, sands and clay (Akujieze, 2004). The sedimentary sequences are poorly bedded with discontinuous clay horizons at various depths. It is estimated to be about 800m thick under Benin City and about 1,830m near the sea shore sections of the formation. They are exposed at various erosion sites, sand quarry sites, and road cuttings. The Benin formation covers 95% of the region, (Anyanwu et al., 2022).

1.3 Alluvium

These are found along Ikpoba and Ovia flood plains. They are made up of grayish-dirty white-yellowish-white sands, silts, clayey sands, gravels and even wood-plant materials. These have been washed down the river valley and deposited at the river banks; they are recent deposits, (Ikhile, 2016).

1.4 Drift/Top Soil

Drifts are sediments still in the process of transportation or movement. They are made up of light brown-yellowish silt, mudflows and sands derived from the weathering of the parental Benin Formation. Drifts are washed down by fluvial agents especially the storms and floods dominating the wet season of the region. The drifts are not part of the solid geology. But they are mainly derived and reworked materials and loads dropped by moving floods, (Adegoke and Akande, 2017). Drifts cover roadsides; fill up areas, concealing the underlying geology. Drifts vary from very thin veneers to up to 0.55 m. The drifts cover about 2% of the urban area. Where the drifts are stabilized soil profile formation is developed.

1.5 Azagba-Ogwashi (Asaba-Ogwashi) Formation

The Azagba-Ogwashi formation has been missing spelt as Ogwashi-Asaba formation (Reyment, 1965), It consists of clays, sands and grits and seams of lignite alternating with gritty clays. It grades upwards into the Benin Formation. The Ogwashi-Asaba formation is exposed in stream channels at the northern parts of the Benin Region, west of Ekiadolor-Iwu and 4 km east of Utekon and north of Azalla, (Akujieze, 2004).

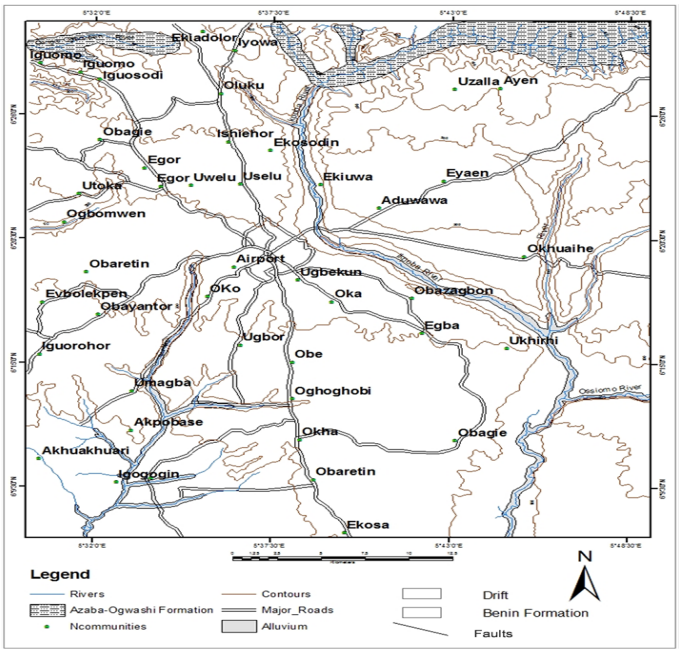

Figure 1: Benin region geological formation (After Akujieze, 2004).

1.6 Location of the Study Area

The study area is Obedolougbeyi and Idogbo Sapele Bypass region, Benin. The area is highly accessible with major and minor roads, together with other adjoining roots. The location geological map (Figure 2) was generated using the global positioning system (GPS) co- ordinates obtained from the field studies together with the field photographs (Figure 3)

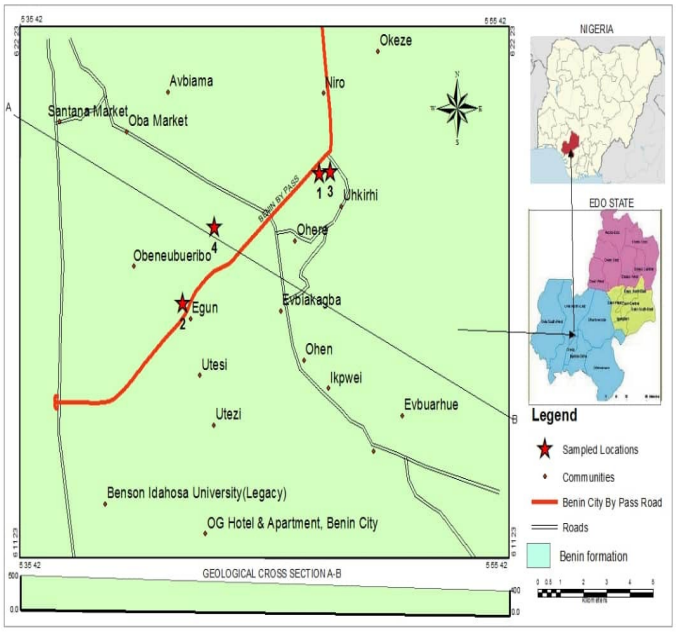

Figure 2: Geological map of study area.

Figure 3: Field photograph for the study locations at Idogbo and Obedoluogbeyi

2. Materials and Method

2.1 Materials

Methods of investigation involved both field study and laboratory analyses.

Forty (40) fresh sediment outcrop samples were collected from Obedolougbeyi and Idogbo along sapele bypass in Benin Region, Edo state. Chip and Grab sampling methods were adopted. Hammer, chisel, GPS, and sample bags were used. The collected samples were analysed using ICP-MS.

2.2 Methods

2.2.1 Major Oxide Analysis (X-ray Flourescence)

Seven (7) samples consisting of eleven (11) major oxides were analyzed (SiO_2, TiO_2, Al_2O_3, Fe_2O_3, MnO, MgO CaO, Na_2O, K_2O and P_2O_5) using Axios instrument with a 2.4 kWatt Rh X- ray Tube. Further, the same set of samples was also analyzed for trace element using LA-ICPMS instrumental analysis; LA- ICP-MS is a powerful and sensitive analytical technique for multi-elemental analysis. The laser was used to vaporize the surface of the solid sample, while the vapour and any particles, were transported by the carrier gas flow to the ICP-MS. The detailed procedures for sample preparation for both analytical techniques are reported below.

- Add 10.0000 g ± 0.0009g Claisse flux and fuse in M4 Claisse fluxer for 23 minutes.
- 0.2 g of $NaCO_3$ was added to the mix and the sample+flux+$NaCO_3$ was pre-oxidized at 700°C before fusion.
- Flux type: Ultrapure Fused Anhydrous Li-Tetraborate-Li- Metaborate flux (66.67 % $Li_2B_4O_7$ + 32.83 % $LiBO_2$) and a releasing agent Li-Iodide (0.5 % LiI).

2.2.2 Pressed Pellet Method for Trace Element Analysis

- Weigh 8g ± 0.05 g of milled powder
- Mix thoroughly with 3 drops of wax binder
- Press pellet with pill press to 15-tonne pressure
- Dry in oven at 100°C for half an hour before analysing.

Five (5) trace elements (Ba, Cr, Zn, Mn, Cu) were analysed using Phillips PW-1800 X-ray fluorescence (XRF) analyzer.

2.3 Inductively Coupled Plasma- Mass Spectrometre (ICP-MS) for Rare Earth Elements (REE) Analysis

Seven (7) samples were analysed for REE. The ICP-MS measurement was conducted using a PerkinElmer Nexion 300 ICP-MS system. In the measurement, the primary REE interferences were oxides of lighter elements. The detection limits for REE are in the level of 0.5 to 5 parts per trillion (ppt), according to (Deng et al., 2022) procedure. The REE mixture standard was used (MilliporeSigma; periodic table mix 3 for ICP. In the analyses, the standards were in the concentration range of 1 to 1000 parts per million. All the analyzed samples were carefully diluted into the concentration range, which is at least two orders of magnitude higher than the detection limit of quantification.

3. Results and Discussion

The results obtained from the geochemical studies are systematically presented. These results have been presented in the order in which the analysis was done and represented using tables, charts, bivariate plots, and scatter plots all geared towards easy and comprehensive data interpretation.

3.1 Results

The data obtained from geochemical analysis of each sample were presented in the form of tables, charts and scatter plots. The maturity, provenance and source area weathering has been sequentially discussed in the section that follows.

3.2 Geochemistry of the major oxide of the sediment

Table 1: Major Oxides Geochemistry of the Coastal Plain Sand

Sample No	SiO_2 (%)	Al_2O_3 (%)	Fe_2O_3 (%)	TiO_2 (%)	CaO (%)	P_2O_5 (%)	K_2O (%)	MnO (%)	MgO (%)	Na_2O (%)	LOI
IDG 1	73.30	12.17	6.20	1.80	0.19	0.21	2.07	0.06	0.20	0.30	3.50
IDG 2	72.10	13.23	4.09	0.40	2.30	0.25	2.30	0.03	0.35	2.05	2.90
IDG 3	70.23	11.08	9.03	1.45	0.32	0.04	2.67	0.03	0.39	0.45	4.31
OBY 11	71.32	10.76	6.67	0.21	0.34	0.39	4.20	0.05	0.10	2.76	3.20
OBY 12	70.52	10.59	6.20	0.19	0.93	0.32	1.71	0.07	0.97	2.21	4.29
OBY 13	71.09	11.01	7.00	0.40	1.66	0.07	2.09	0.04	0.62	2.76	3.00
OBY 14	73.67	12.34	4.55	0.45	1.32	0.04	1.06	0.03	0.52	2.45	2.91

Data from Table 1 of the major oxides show that seven (7) samples consisting of ten (10) major oxides were analysed in percentage (%) as follows: SiO_2 ranged 70.23-73.69 (~71.70); Al_2O_3 ranged 10.59-13.23 (~11.60); Fe_2O_3 ranged 4.09-9.03 (~6.20); TiO_2 ranged 0.40-1.80 (~0.70); CaO ranged 0.19-2.30 (~1.00); P_2O_5 ranged 0.04-0.36 (~0.78); K_2O ranged 1.06-4.20 (~2.30); MnO ranged 0.03-0.070 (~0.04); MgO ranged 0.10-0.97 (~0.45); Na_2O ranged 0.30-2.76 (~1.85). The low concentration of Fe_2O_3, Al_2O_3 and TiO_2 (Table 1) could be due to chemical disintegration under oxidizing conditions during weathering and diagenesis.

It can also be observed that: $SiO_2 > Al_2O_3 > Fe_2O_3 > K_2O > Na_2O > CaO > TiO2 > MgO > P_2O_5 > MnO$ in percentage abundance (Table 1) and this is corroborated by Figure 4 which clearly shows their variation.

The concentration of SiO_2 (~71.7%) can be associated with the presence of quartz particles being the highest in value for all the understudied samples and it refers to the higher sand fraction in particle size distribution analysis and higher quartz content in mineral composition which is indicated by the values of this study. SiO_2 strongly resists weathering because it is mainly contained in quartz minerals. Quartz is well enriched in felsic igneous rocks (Nzeukou *et al.,* 2021). With an average of 71.7%, the major element results of the tested samples revealed that the plain sands are highly rich in SiO_2 (silica), which is higher than the norm of 66% by weight for upper continental crust (UCC) (Omoruyi et al., 2023).

Al_2O_3 reflects the presence of aluminosilicates (~11.60%). Al_2O_3 is mainly is less resistant to weathering owing to its presence in clay materials; a high percentage concentration of Al_2O_3 indicates a high content of clay present in a sample (Dengiz et al., 2019); the values of Al_2O_3 being low (10.59-13.23%) recorded in this work are indicative of low clay content present in the samples.

In Table 4.1, the presence of hematite can be correlated with the abundance of iron (Fe_2O_3; ~6.20%). Fe_2O_3 being > 2 is probably responsible for the extreme changes in colour as seen in the coastal plain sands from pink, yellow to red and the deposition of iron minerals (Nzeukou et al., 2021).

TiO_2 (~0.70%; Table 1) of this average suggests that a higher portion if the heavy mineral, rutile indicating stronger weathering regimes. Being coastal plain sands, CaO (~1.00%) indicate a depositional influence of marine carbonate sediments or erosion of pre-existing carbonate formations; also, less weathered sands retain higher percentage of CaO (Dengiz et al., 2019).

P_2O_5 (~0.78%; Table 1) is generally low when compared to typical agricultural soils and this has implications of limited plant growth on such soils. Again, intense weathering can lead to leaching of phosphorus from the soil potentially explaining the low values obtained (Hoque and Roy, 2019). K_2O (~2.30%; Table 1) has a significant implication as having originated from potassium feldspar-rich sediments and thus good for agriculture. This value also shows that leaching of this oxide was minimized (Adeila et al., 2019). MnO (~0.04%; Table 4.1) in coastal plain sands can be associated with other potentially harmful heavy metals. MgO (~0.45%) indicate past marine influence on the deposition of the coastal plain sands and that it has been involved in various diagenetic processes in sediments. Na_2O (~1.85%; Table 4.1) is of significant value indicating marine influences and high saline intrusion from seawater. This value has significant influence also on soil pH pushing it towards alkalinity (Nzeukou et al., 2021).

3.3 Mineral Association among the Major Oxides from the Correlation and Chi-square

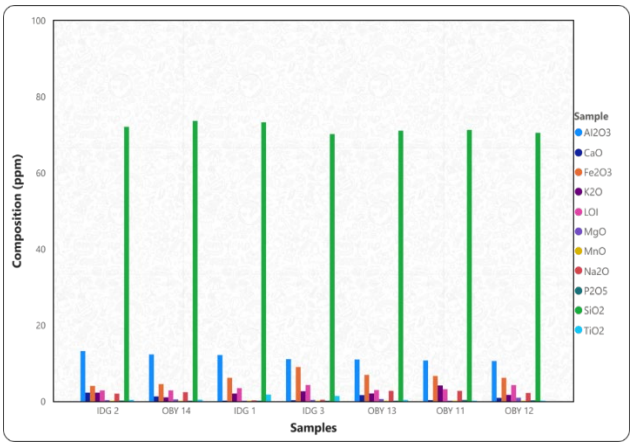

Figure 4: Variation in the major oxide Composition

We assume that any two oxides we investigate share a common behaviour in the absolute deviation of their percentage composition from a mean value. That is to say that a change in one oxide will almost certainly necessitate an equivalent change in the corresponding oxide, (Figure 4). This may likely be due to a substitution reaction between oxides during formation of the rock where an oxide initially present is slowly replaced by another, causing a negative correlation value. This is typical of the correlation of SiO_2 versus Fe_2O_3 and Al_2O_3 versus Fe_2O_3 refer to figures (5 and 6) accordingly.

Alternatively, it could also mean one oxide has high affinity for the other and therefore tend to occur together naturally even prior to the formation of the rock from which the sample was collected. In such a scenario, absolute changes of both percentage compositions correlate positively. The two oxides also show a strong positive correlation that supports the position of the chi-squared test. Both tests indicate there may be a common latent property between both components, perhaps a natural affinity for each other or mutual passivity. This is typical of the correlated results of Al_2O_3 versus SiO_2, TiO_2 versus Al_2O_3 and TiO_2 versus SiO_2 and pertains to Figures (5, 6 and 7).

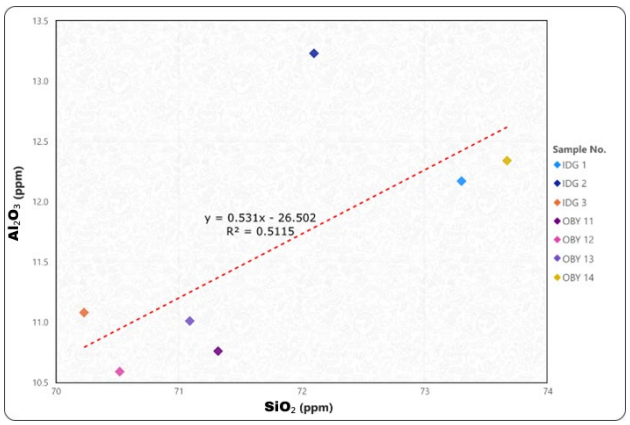

Figure 5: Scatter plot of Al_2O_3 versus SiO_2 for the coastal sand

Table 2: Correlation and Chi square of SiO_2 and Al_2O_3		
Correlation	***Al_2O_3***	***SiO_2***
Al_2O_3	1	
SiO_2	0.715	1
Chi-Square		1.02
P-Value		0.31
Critical Value @ 0.05 for Degree of Freedom of 1		3.84

The P-Value (31%) obtained is greater than critical P-Value (5%) suggesting that the null hypothesis does not holds true, (Table 4.2). Conversely, chi square value of 1.02 less than the critical chi square value of 3.84 suggest we reject null hypothesis. In addition, the value of the correlation of Al_2O_3 versus SiO_2 (0.715) shows that they are strongly correlated, showing an excellent relationship between both metallic oxides, (Figure 4.2).

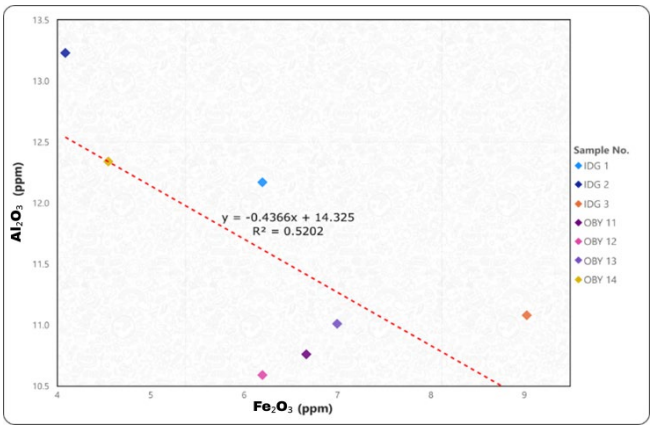

Figure 6: Scatter plot of Al_2O_3 versus Fe_2O_3 of the coastal sand

Table 3: Correlation and Chi square of Fe_2O_3 and Al_2O_3		
Correlation	***Al_2O_3***	***Fe_2O_3***
Al_2O_3	1	
Fe_2O_3	-0.721	1
	Chi-Square	14.87
	P-Value	0.0001
	Critical Value @ 0.05 for Degree of Freedom of 1	3.84

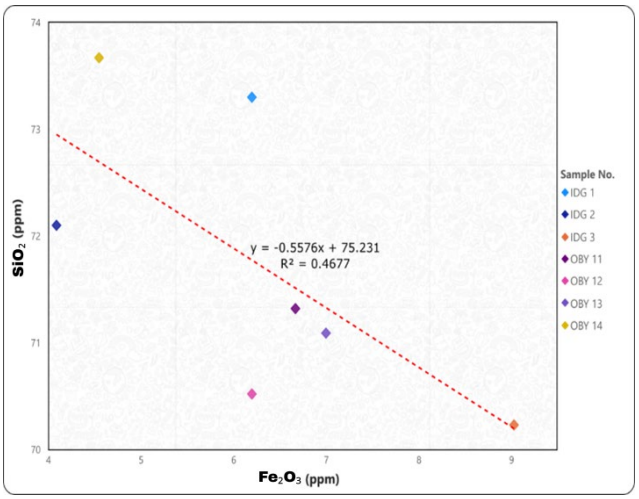

Figure 7: Scatter plot of SiO_2 versus Fe_2O_3 for the coastal sand

The P-Value (0.01%) obtained is less than critical P-Value (5%) suggesting that the null hold true (Table 3). Conversely, chi square value of 14.87 greater than the critical chi square value of 3.84 suggests we accept null hypothesis. The strong negative (Figure 5) correlation might suggest a substitutive relationship but without the chi-squared test to support the position there is no guarantee of exclusivity in that relationship. That is to

say the substitution of one Al_2O_3 might be carried out by multiple other oxides including the one under investigation that is Fe_2O_3.

Table 4: Correlation and Chi square of Fe_2O_3 and SiO_2

Correlation	SiO_2	Fe_2O_3
SiO_2	1	
Fe_2O_3	-0.684	1
Chi-Square		59.4
P-Value		1.28×10^{-14}
Critical Value @ 0.05 for Degree of Freedom of 1		3.84

The P-Value (~0%) obtained is less than critical P-Value (5%) suggesting that the null hypothesis holds true (Table 4). Conversely, chi square value of 59.40 greater than the critical chi square value of 3.84 suggests we accept null hypothesis

The weak negative correlation (Figure 7) might suggest a substitutive relationship but without the chi-squared test to support the position there is no guarantee of exclusivity in that relationship. That is to say the substitution of one oxide might be carried out by multiple other oxides including the one under investigation.

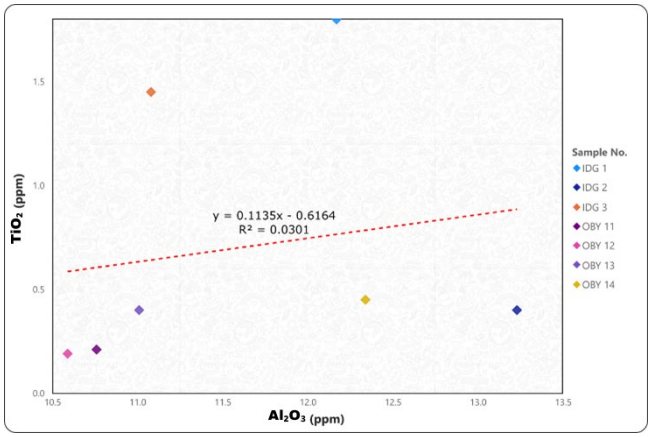

Figure 8: Scatter plot of TiO_2 versus Al_2O_3 for the coastal sand

Table 5: Correlation and Chi square of Al_2O_3 and TiO_2

Correlation	TiO_2	Al_2O_3
TiO_2	1	
Al_2O_3	0.173	1
Chi-Square		0.03
P-Value		0.86
Critical Value @ 0.05 for Degree of Freedom of 1		3.84

The P-Value (86%) obtained is significantly greater than critical P-Value (5%) suggesting that the null hypothesis does not hold true (Table 5). Conversely, chi square value of 0.03 less than the critical chi square value of 3.84 suggests we reject null hypothesis. However, a poor positive correlation might suggest a weak affinity of both oxides.

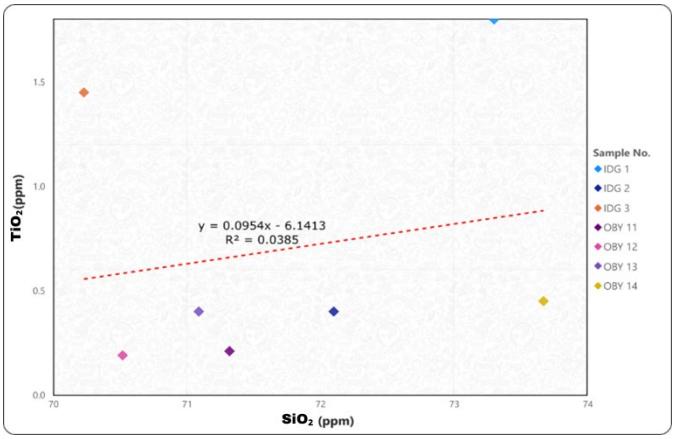

Figure 9: Scatter plot of TiO_2 versus SiO_2 for the coastal sand

Table 6: Correlation and Chi square of SiO_2 and TiO_2		
Correlation	***TiO_2***	***SiO_2***
TiO_2	1	
SiO_2	0.196	1
Chi-Square		0.03
P-Value		0.86
Critical Value @ 0.05 for Degree of Freedom of 1		3.84

The P-Value (86%) obtained is significantly greater than critical P-Value (5%) suggesting that the null hypothesis does not holds true (Table 6). Conversely, chi square value of 0.03 less than the critical chi square value of 3.84 suggests we reject null hypothesis. However, a poor positive correlation might suggest a weak affinity of both oxides (Figure 8).

3.4 Source Area Weathering of the Coastal Sand

Weathering is described as the physical and chemical alteration of rocks and minerals on or near the Earth's surface (Ejeh, 2021). Chemical decomposition of rocks due to weathering results in the enrichment of Al_2O_3 and depletion of the alkalis (Na_2O, K_2O, CaO, and MgO). Chemical weathering indices estimate the intensity of soil chemical weathering by comparing changes in major and trace metal concentrations as ratios of mobile to immobile elements in soil and rock or parent material (Nesbitt and Young, 1982). Water and oxygen are important to many chemical weathering reactions.

Table 7: Weathering indices of the coastal plain sand								
Weathering Indices	*IDG 1*	*IDG 2*	*IDG 3*	*OBY 11*	*OBY 12*	*OBY 13*	*OBY 14*	*AVERAGE*
PIA	95.10	69.0	91.60	68.00	73.90	66.90	75.00	77.07
CIA	82.60	64.70	15.61	59.70	68.60	62.80	71.00	61.40
CIW	96.10	75.30	93.50	90.80	77.10	71.30	76.60	83.00
MIA	65.20	29.40	68.78	19.40	37.20	25.60	42.00	41.10

For the weathering indices (Table 7) the chemical index of alteration (CIA) values ranged 15.61-82.60 (~61.40); the chemical index weathering (CIW) had ranging values of 71.30-96.10 (~83.00); the plagioclase index of alteration (PIA) had values ranging from 66.90-96.10 (~77.07) and the mineralogy index of alteration (MIA) had values ranging from 25.60-68.78 (~41.10).

The CIA monitors the progressive transformation of potassium feldspars and plagioclase into clay minerals. The CIA is based on the assumption that the relative abundance of major elements in a rock change as a result of weathering, with more resistant elements (such as quartz) is becoming more abundant and more easily weathered elements (such as feldspars) becoming less abundant. Calculating the Chemical Index of Alteration (CIA), where CIA = molar (Al_2O_3/[Al_2O_3+CaO+Na_2O+K_2O]) x 100, can help understand the extent of chemical weathering of the sediments' source rocks, according to Nesbitt and Young, (1982).

According to Nesbitt, stages of weathering were given as follows: weathering at the incipient stage is indicated by CIA value of 30-55, weathering at the intermediate stage is represented by CIA value of 51-85, and weathering at the advanced stage is indicated by CIA values greater than 85.

According to the study, the CIA can also be applied in palaeo-climatic reconstruction as follows: the CIA spectra of 50–60 indicate low chemical weathering, 60–80 suggests moderate chemical weathering (in cool and/or arid climate), and 80–100 implies intensive chemical weathering (in hot and/or humid climate) (Nesbitt and Young, 1982; McLennan et al., 1993; Dengiz et al., 2019; Ejeh, 2021).

The CIA range (15.61-82.60) showed that all of the samples were at the intermediate stage of weathering with the exception of one sample location (OBY and IDG) having advanced chemical weathering. However, the average CIA value for all the samples examined had an average of 61.40 indicating weathering at an intermediate stage, moderate chemical weathering and the paleo-climatic conditions were cool and/or arid (Table 4.7). The paleo-climatic conditions of this study agree with Omoruyi et al., (2022).

In understanding the CIW, the only difference between the CIA and the Chemical Index of Weathering (CIW) proposed by Harnois (1988) is the omission of K_2O from the equation: CIW = molar [(Al_2O_3 / (Al_2O_3+ CaO + Na_2O)] x 100. Chemical Index of Weathering (CIW) values range from 50 for unweathered upper continental crust to roughly 100 for materials that have undergone substantial weathering, with the full elimination of alkali and alkaline-earth elements [McLennan (1993), Mongelli *et al.,* (1996)]. CIW in this investigation had an average value of 83.00 signifying that the samples had undergone a significant level of substantial weathering at the time of this study.

PIA is similar to CIA but focuses specifically on the alteration of plagioclase feldspar (Ilevbare and Omoruyi, 2020). The intensity of the chemical weathering can also be estimated using the Plagioclase Index of Alteration (PIA); in molecular proportions: PIA = [(Al_2O_3-K_2O)/(Al_2O_3 + CaO* + Na_2O-K_2O)] × 100 where CaO* is the CaO residing only in the silicate fraction and calculated as CaO* = ¼ CaO -10/3 * P_2O_5 (McLennan *et al.,* 1993). Unweathered plagioclase has PIA value of 50 while Phanerozoic samples have PIA value of 79. Fedo *et al.,* (1995) suggested the Plagioclase Index of Alteration (PIA) as an alternative to the CIW. The PIA can be used to track plagioclase weathering because it dissolves quite quickly and is ubiquitous in silicate. PIA in this study had an average of 77.07 indicating that the samples were Phanerozoic (Table 4.7).

In order to determine the mineralogical index of alteration (MIA), MIA = 2* (CIA-50). In order to evaluate MIA values, it is helpful to consider the following ranges: incipient (0–20%), weak (20–40%), moderate (40–60%), and intense to extreme (60–100%) degree of weathering (Omoruyi et al., 2022). With an average value of 41.10, it could be inferred that the samples had undergone moderate degree of weathering thus, corroborating the result gotten from the PIA (Table 4.7).

3.5 Provenance of the Coastal Sand

The geochemical attributes of elements and their ratios (major and trace elements) in coastal plain sands can be used invaluably for construing provenance (Oti and Nwachukwu, 2021).

Table 8: Significant ratios of major oxides of Obedoluogbeyi and Idogbo coastal plain sand								
Major Oxides Ratios	IDG 1	IDG 2	IDG 3	OBY 7	OBY 12	OBY 13	OBY 14	AVERAGE
SiO_2/Al_2O_3	6.02	5.45	6.34	6.63	6.66	6.46	5.97	6.22

Table 8 (cont): Significant ratios of major oxides of Obedoluogbeyi and Idogbo coastal plain sand								
Fe_2O_3/K_2O	3.0	1.78	3.38	1.59	3.63	3.34	4.29	3.00
Al_2O_3/TiO_2	6.76	33.08	7.64	51.23	51.23	55.74	27.53	29.9
K_2O/Na_2O	6.9	1.12	5.93	1.52	1.77	0.76	0.43	2.49
K_2O/Al_2O_3	0.17	0.17	0.24	2.39	0.16	0.19	0.09	0.49

In Table 8, the averages of SiO_2/Al_2O_3, Fe_2O_3/K_2O, Al_2O_3/TiO_2, K_2O/Al_2O_3 are 6.25, 37.06, 194.70 and 0.23 respectively with Al_2O_3/TiO_2 being the highest and K_2O/Al_2O_3 being the lowest (Al_2O_3/TiO_2 > Fe_2O_3/K_2O > SiO_2/Al_2O_3 > K_2O/Na_2O > K_2O/Al_2O_3). These ratios are useful in provenance and maturity determination. SiO_2/Al_2O_3 ratios in unaltered igneous rocks range from ≈3.0 for basic rocks to ≈5.0 for acidic rocks (Roser et al., 1996). Results from this study SiO_2/Al_2O_3 averages 6.22 show that the coastal plain sands were weathered from acidic rocks (Table 8).

Al_2O_3 was greatly enriched in the soil samples compared to TiO_2 (Table 4.8). Some previous works have reported Al_2O_3/TiO_2 ranges of 3–8, 8–21, and 21–70 for mafic-igneous, intermediate, and felsic sources respectively (Girty et al., 1996; Opara et al., 2021). The average (~29.90) reported indicated here in this study infers that the coastal plain sands are sourced from felsic rocks. This inference is supported by the SiO_2 (~71.74%) value obtained in Table 4.6 reflecting a high silica content for the coastal plain sand. Fe_2O_3/K_2O (1.59-4.29; ~3.00) showed that there was relatively higher deposition of iron oxide compared to potassium oxide. According to Adeila et al., (2019), the presence of haematite denotes an oxidizing environment and thus suggesting that a humid climate prevailed in the area during the period of deposition. Hence, it can be inferred that the high ratio of iron oxide indicates abundant deposition of haematite, strong oxic environment and humid climate.

Also, samples with low SiO_2/Al_2O_3 ratio and a higher Fe_2O_3/K_2O ratio are mineralogical less stable and more prone to reactivity during supercritical CO_2 exposure (Farquhar et al., 2014). K_2O/Na_2O >1 signify that K–feldspar is the dominant source rock and enrichment of K_2O is associated with the illite clay mineral in these coastal plain sands (Ilevbare and Omoruyi 2020b).

The average low values of K_2O/Al_2O_3 (0.49) point to likely increased source area weathering or sedimentary recycling (Bauluz et al., 2000). K_2O/Al_2O_3 very low values indicates burial diagenesis was probable and this also points to likely increased source area weathering or sedimentary recycling (Bauluz et al., 2000; Ghosh et al., 2019). K_2O was not greatly enriched in the soil samples compared to Al_2O_3 (Table 6).

3.6 Maturity of the Coastal Sand from Geochemical Characteristics

Maturity of sands can be reflected by the SiO_2/Al_2O_3 index. High ratios indicate mineralogical mature samples, while low ratios represent chemically immature samples (Haque and Roy, 2019). An average value of 6.22 indicates that the samples are mineralogical immature (Table 8).

Low values of K_2O/Al_2O_3 indicate low sediment maturity (Ilevbare and Imasuen, 2020). K_2O/Al_2O_3 values of ~0.23 in this study rightly suggest low sediment maturity (Table 8). Low values for both SiO_2/Al_2O_3 and K_2O/Na_2O ratios indicate mineralogical immature sediments.

3.7 Geochemistry of the Trace Elements of the Sediment

The relative abundance of trace elements and oxides in sediment is controlled by sedimentation rate, terrigenous influx, biogenic influx, hydrothermal input, diagenesis and, ultimately, weathering. Their enrichments can lead to understanding of their paleo-depositional and paleo redox setting, as well as the paleo-climate, (Ghosh et al., 2019).

From Table 9 above, it can be observed that ten (11) trace elements were studied and analysed, and their values are given in ppm: Ni (19-110; ~39), Cs (32-320; ~81), Co (33-215; ~58); Sr (57-322; ~72), Cr (35-94; ~38), Ba (52-600; ~123), Ta (31-72; ~33), Nb (22-110; ~42), Sc (26-72; ~23), Nd (11-95; ~44) and Y (20-65; ~23).

High concentrations of Ba even as seen in the results of this study indicate the presence of marine depositional environment (Zhang et al., 2021). According to the studyNi concentrations larger than 200 ppm signs of mafic or ultramafic provenance (Gao et al., 2020). Ni with an average of 39 ppm indicates that the Idogbo and Obedoluogbeyi coastal plain sand are of felsic origin.

As suggested that when Cr is greater than 150ppm in abundance, it is an indication of mafic or ultramafic provenance (Omoruyi et al., 2022). The highest recorded value of Cr in this study is less than the stated value (ave. 34 ppm) indicating a felsic provenance relative to the above conditions.

According to the study elements like Sc, Cr, Ni and Co are suitable for provenance and tectonic setting determination because of their very limited mobility throughout sedimentary processes, and their brief durations in saltwater, as a result of their quantitative transit into clastic deposit during weathering and transport, these components serve as a proxy for the parent material (Zhang et al., 2021; Gu et al., 2021).

Table 9: Trace element Geochemistry of the coastal plain sand

Sample No.	Ni (ppm)	Cs (ppm)	Co (ppm)	Sr (ppm)	Cr (ppm)	Ba (ppm)	Ta (ppm)	Nb (ppm)	Sc (ppm)	Nd (ppm)	Y (ppm)
IDG 8	32	112	123	67	35	600	50	43	29	78	24
IDG 9	75	133	33	64	65	70	54	93	26	95	44
IDG 10	27	320	215	78	66	52	31	22	30	76	32
OBY 14	88	162	71	66	72	70	52	77	26	95	20
OBY 15	19	88	52	57	35	231	59	49	25	67	30
OBY 16	76	43	63	66	94	120	56	72	45	59	33
OBY 17	110	32	79	322	49	212	72	110	72	11	65

3.8 Geochemistry of the Rare Earth Element (REE) of the Sediment

The Periodic table elements from lanthanum (La: Z = 57) to lutetium (Lu: Z = 71) are usually referred to as rare earth elements (REEs). The REEs, also known as Lanthanides or 'Industrial vitamins', are a chemically uniform metallic group of elements having almost similar electronic configuration, including the same electronic layers but with small differences in their atomic number (Hossain et al., 2023). RREs are known as 'rare' not because they are exceptionally uncommon, but are not found in economically available deposits (Mirkouei et al., 2021). There are seventeen elements in the group of REEs: cerium (Ce), dysprosium (Dy), erbium (Er), europium (Eu), gadolinium (Gd), holmium (Ho), lanthanum (La), lutetium (Lu), neodymium (Nd), praseodymium (Pr), samarium (Sm), terbium (Tb), thulium (Th), ytterbium (Yb) (Khan et al., 2017; Balaram, 2019). The REE in the samples analysed, their concentration and how they varied are presented (Table 10; Figure 10).

Table 10: Rare earth elements Geochemistry of the Coastal Sand

Sample No.	Gd (ppm)	Tb (ppm)	Y (ppm)	Yb (ppm)	La (ppm)	Ce (ppm)	Pr (ppm)	Nd ppm)	Sm (ppm)	Eu (ppm)
IDG 12	0.25	0.16	0.16	0.21	6.0	15.91	1.9	6.4	8.2	0.22
IDG 13	1.47	0.13	0.19	0.19	7.9	16.30	1.7	4.7	9.0	0.17
IDG 14	1.21	0.17	0.26	0.14	9.3	18.00	1.9	3.4	7.2	0.19
OBY 17	0.96	0.15	0.17	0.15	6.7	15.12	1.4	7.1	9.2	0.38
OBY 18	1.38	0.10	0.20	0.06	7.0	16.20	1.5	6.4	8.3	0.32
OBY 19	1.42	0.19	0.12	0.17	7.3	13.90	1.0	6.2	4.4	0.19
OBY 20	1.32	0.19	0.23	0.12	8.3	16.45	1.6	5.5	9.2	0.15

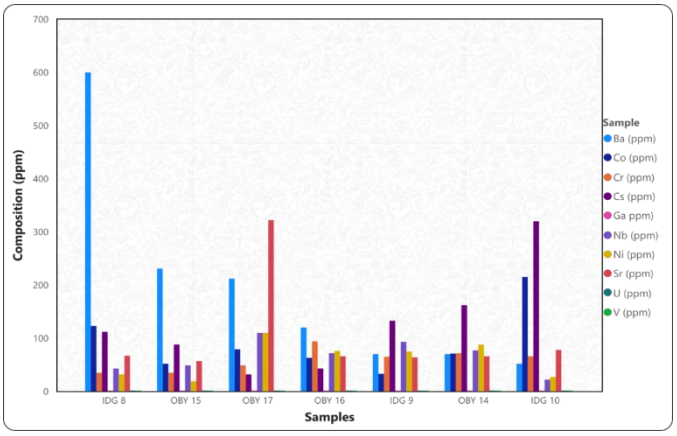

Figure 10: Variation in the trace elements of the coastal plain sand

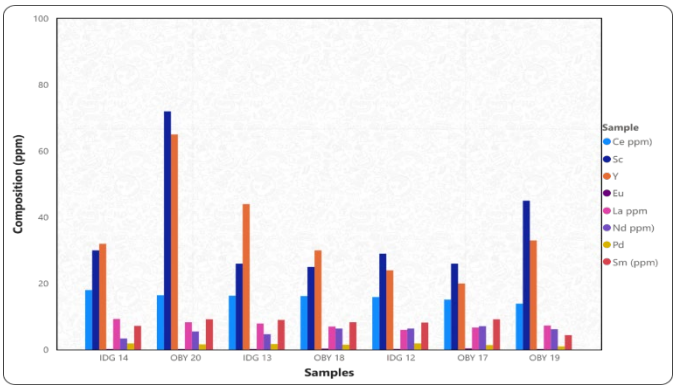

Figure 11: Variation in the rare earth elements of the coastal sand

Nd is extensively applied in super magnets for disk drives, Ce is critical ingredient in autocatalyts and all REE are used in making the flat-panel TVs. Eu is notable for its use in phosphors which are applied in coloured television tubes and LED screens that emit red and blue lights (Guo et al., 2021). Several compounds of REE are in smart-batteries that power every electric vehicle and hybrid electric vehicles. Because of their unique physical, chemical, magnetic, luminescent properties, these elements help to make many technological advantages such as performing at reduced energy consumption, greater efficiency, miniaturization, speed, durability and thermal stability (Balaram, 2019; Hossain et al., 2023). Sm is often used in the production of highly stable and strong magnets even at elevated temperatures which are thus used in electronic devices, motors, etc. Pr is often used in alloys for making permanent magnets, in combination with neodymium for electric motors and generators (Al-Maadhidi et al., 2023). La is used in the production of certain types of catalysts, as well as in the manufacturing of high-performance alloys; these are used in production of optical lenses, phosphors, and other electronic devices (Saleh et al., 2023). Though not being part of the lanthanide series, Y is often associated with the rare earth elements because of its similar occurrences with them. It is used in the production of phosphors, medical imaging devices and superconductors. Just like Y, Sc is not regarded as a rare earth element but has useful applications in the production of light-weight alloys for the aerospace industry (He et al., 2023; Lohr et al., 2024).

4. Conclusion

The following conclusion stems from this study;

- The provenance of the coastal sand was of felsic igneous origin;
- Weathering condition that prevailed is Humid Climate and the sediment have undergone substantial to intense chemical weathering;
- The Sand from the major oxide geochemistry is Mature;
- The Correlation and Chi-square of the metallic oxides shows enrichment of silica and depletion of other oxides as well as indicates a common source of for the coastal plain sand.
- The coastal sand in Sapele Bypass is most likely to be a reservoir rock for hydrocarbon potential, if the it is in a petroleum system with source and trap rather than a source rock.

Declarations

Competing interests, the authors declare no competing interest.

References

Adegoke, O. A., and Akande, O. A. 2017. Sedimentology and sequence stratigraphy of the Agbada Formation, Niger Delta: implications for hydrocarbon prospectivity. Journal of African Earth Sciences, 138, 101-119.

Adiela, U.P., Jackosn, C.A., Moses, A. 2019. Sedimentology and Depositional

Enviroment of Ajali Sandstone, Anambra Basin, Southern Nigeria. https://www.researchgate.net/publication/338210042

Ajadi, J., Yusuf, A.J., Ajala, A.A. 2020. Sedimentological characterization of clastic sediments of Anambra basin: implications for provenance and paleo-environments. Research gate.

Ajakaiye, D. O., and Oti, M. O. 2016. Tectonic evolution of the Niger Delta basin: implications for hydrocarbon exploration. Journal of Petroleum Geology, 39(2), Pp. 147-163

Akinyemi, S. A., Adebayo, O. F., and Ojo, A. O. 2015. Paleoenvironmental studies of Odagbo coal mine sequence, northern Anambra basin, Nigeria: Insight from Palynomorph and geochemical analyses. International Journal of Current Research, 7 (9), Pp. 20274- 20286

Akujieze, C.N. 2004. Effects of Anthropogenic Activities (Sand Quarrying and Waste Disposal) on Urban Groundwater System and Aquifer Vulnerability Assessment in Benin City, Edo State, Nigeria. PhD Thesis, University of Benin, Benin City, Nigeria.

Al-Maadhidi, A.S., Kadhim, L.S., Alkhafaji, M.W. 2023. Trace and Rare Earth Elements Geochemistry of the Mudstone Rocks from Injana Formation: Implications for Provenance and Paleoclimate. The Iraqi Geological Journal, Pp. 159-174.

Anyanwu, T.C., Ekpo, B.O., Oriji, B.A. 2022. Biomarker Application in the Recognition of the Geochemical Characteristics of Crude Oils from the Five Depobelts of the Niger Delta Basin, Nigeria. Iranian Journal of Earth Sciences. Vol. 14, No. 1, 2022, Pp. 1-17. DOI: 10.30495/ijes.2022.1943029.1664

Balaram, V. 2019. Rare Earth Elements: A Review of Applications, Occurrence, Exploration, Analysis, Recycling, and Environmental Impact. Elsevier; Geoscience Frontiers 10, 1285-1303. CSIR - National Geophysical Research Institute, Hyderabad 500 007, India

Bauluz, B., Mayayo, M. J., Fernandez-Nieto, C., and Gonzalez Lopez, J. M. 2000. Geochemistry of Precambrian and Paleozoic Siliciclastic Rocks from the Iberian Range (NE Spain): Implications for Source-area Weathering, Sorting, Provenance, and Tectonic Setting. Chemical Geology, 168(1), Pp. 135-150. http://dx.doi.org/10.1016/S0009-2541(00)00192-3

Boboye, O.A., Chidiebere, C. 2023. Sedimentological and palynological assessment of three wells in Eastern Dahomey Embayment, southwestern Nigeria, West Africa. Quarternary international 657, Pp. 77-91.

Deng, B., Wang, X., Luong, D. X., Carter, R. A., Wang, Z., Tomson, M.B., Tour, J. M. 2022. Rare Earth Elements from Waste. Chemistry: Science Advances; Research Article.

Dengiz, O., Tunçay, T., Bayramin, I., Kilic, S., Baskan, O. 2019. Chemical weathering indices applied to soils developed on old lake sediments in a semi-arid region of Turkey. Eurasian journal of soil science. DOI: 10.18393/ejss.499122

Dickinson, W. R. 1983. Interpreting detrital modes of Greywacke and Arkose. Sedimentary Petrology Journal, 40, 695-707.

Ejeh, O. I. 2021. Geochemistry of rocks (Late Cretaceous) in the Anambra Basin, SE Nigeria:insights into provenance, tectonic setting, and other palaeo-conditions https://doi.org/10.1016/j.heliyon.2021.e08110

Farquhar, et al., 2014. A Fresh Approach to Investigating CO_2 Storage: Experimental CO_2- Water-rock Interactions in a Low-salinity Reservoir System, Chemical Geology. Pp. 1-70.

Fedo, C.M., Nesbitt, H.W., Young, G.M. 1995. Unraveling the effects of K metasomatism in sedimentary rocks and paleosols with implications for palaeo-weathering conditions and provenance. Geology 23, Pp. 921–924.

Gao, X., Zhang, X., Zhu, X. 2020. Provenance and Tectonic implications of palezoic strata in the south yellow sea Basin, China Reveled from the Bore hole CSDP – 2. Journal of ocean university of China, 19, Pp. 536 – 55

Ghosh, S., Mukhopadhyay, J., Chakraborty, A. 2019. Clay Mineral and Geochemical Proxies for Intense Climate Change in the Permian Gondwana Rock Record from Eastern India. Research Article. Article ID 8974075, 14 pages https://doi.org/10.34133/2019/8974075

Guo, H., Liu, H., Pourret, O., Wang, Z., Sun, Z., Zhang, W., Liu, M. 2021. Distribution of Rare Earth Elements in Sediments of North China Plain: A Probe of Sedimentation Process. Applied Geochemistry 134, 105089.

Haque, M. Md, Roy, M.K. 2019. Sandstone-Shale Geochemistry of Miocene Surma Group in Bandarban Anticline, SE Bangladesh: Implications for Provenance, Weathering, and Tectonic Setting. Earth Sciences. 9(1), Pp. 38-51. doi: 10.11648/j.earth.20200901.15

Haruna, K.A., Ojo, O.J. 2019. Major and trace element evaluation of the Campano-Maastrichtian sediments of Anambra basin exposed around Enugu, Nigeria. Journal of applied sciences and Environmental Management 23 (1), Pp. 111-119.

Hossain, Z.H.M. 2020. Major, trace and REE geochemistry of the Meghna River sediments, Bangladesh: Constraints on weathering and provenance. Geological journal 55 (5), Pp. 3321-3343. https://www.sciencedirect.com/science/article/pii/S1364032121002100

Ighodaro, E.J., Imasuen, O.I., Lucas, F.A., Okiotor, M.E., Uchegbulam, O., Ogueh, E.D., Chigbufue, I.G. 2018. Integrated Sedimentological and Chemostratigraphic Characterisation of OGE-#1 Well, Greater Ughelli Depo-Belt, Niger Delta. Basin. J. Min. Geol. 54(2), 2018. Pp. 149 – 164

Ikhile, C.I. 2016. Geomorphology and Hydrology of the Benin Region, Edo State, Nigeria. International Journal of Geosciences 7, Pp. 144-157. http://dx.doi.org/10.4236/ijg.2016.72012

Ilevbare M., Imasuen O.I. 2020. Sedimentology and maturity of Ajali Formation, Benin flanks Anambra Basin, Nigeria. Ife Journal of Sciences, 22(1): Pp. 123-136. https://doi.org/10.4314/ijs.v22i1.13

Ilevbare M., Omoruyi D.I. 2020. Rare Earth Elements of Ajali Sandstone, SW, Anambra Basin in Nigeria: Implication for Soil Genesis. Journal of Applied Sciences and Environmental Management, 24(11): Pp. 1999-2004. https://dx.doi.org/10.4314/jasem.v24i11.21

Ilevbare M., Omoruyi, D.I. 2020. Trace Elements and Major oxides characteristic of th Geochemistry of Ajali Sandstone, South West, Anambra Basin, Nigeria: Nigerian Journal of Engineering and Environmental Sciences, 5(2): Pp. 737-742. www.rjees.com

Ingersoil, R. V., Bullard, T.F., Ford, R. L., Grim, J. P., Pickle, J.D., and Sares, S. W. 1984. The effects of grain size on data modes: a test of the Gazzi – Dickson point – counting method. Sedimentary Petrology Journal, 46: Pp. 620-632. ISSN 2059-3058

Javed, A., Wahid, A., Mughal, M.S., Khan, M.S., Qammar, R.S., Ali, S.H., Siddiqui, N.A., Iqbal, M.A. 2021. Geological and petrographic investigations of the Miocene molasses deposits in sub-Himalayas, district Sudhnati, Pakistan. Arabian journal of Geosciences 14, Pp. 1-24.

Khan, S.A., Dar, S.A., Khan, K.F., Karim, Y. 2022. Geochemical characteristics of Early Cambrian phosphate bearing sedimentary rocks from the Mussorie syncline, India: Implications for paleo-redox conditions. Geosystems and Geoenvironment 1 (3), 100046.

Kim, P., Anderko, A., Navrotsky, A., Riman, R. 2018. Trends in Structure and Thermodynamic Properties of Normal Rare Earth Carbonates and Rare Earth Hydroxycarbonates. Minerals 8, 106. https://doi.org/10.3390/min8030106.

Liu, Z. 2022. Provenance, source weathering, and tectonic setting of the Lower Cambrian Shuijintuo formation in the middle Yangtze area, China. Marine and petroleum geology 139, 105584.

Lohr, S.C., Spandler, C., Baldermann, A., 2024. Controls on Rapid Rare Earth Element Enrichment in Sediments Deposited by a Continental-scale River System. Geochemica et Cosmochimica Acta 366, Pp. 48-64.

McLennan, S.M., Hemming, S., McDaniel, D.K., Hanson, G.M. 1993. Geochemical approaches to sedimentation, provenance, and tectonics. In: Johnsson, M.J., Basu, A. (Eds.), Processes Controlling the Composition of Clastic Sediments, 284. Geological Society of America. Special Papers, Pp. 21–40.

Meinhold. G., Bassis, A., Hinderer, M., Lewin, A., Berndt, J. 2021. Detrital zircon provenance of north Gondwana Palaeozoic sandstones from Saudi Arabia. Geological magazine 158 (3), Pp. 442-458

Mirkouei, A., Opare, O. E., and Struhs, E. 2021. A Comparative State-of-technology Review and Future Directions for Rare Earth Element Separation. Elsevier.

Mongelli, G., Cullers, R.L., Muelheisen, S. 1996. Geochemistry of Late Cretaceous-Oligocene Shales from the Varicolori Formation, Southern

Apennines, Italy: Implications for Mineralogical, Grain-size Control and Provenance. European Journal of Mineralogy, 8, Pp. 733–754.

Mueller, P., Langone, A., Patacci, M., Giulio, A.D. 2020. Tethyan paleomargin provenance signature: sandstone detrital modes and detrital zircon U-Pb age distribution of the Upper Cretaceous-Paleocene. International journal of earth sciences 109, Pp. 201-220.

Nesbitt, H.W., Young, G.M. 1982. Early Proterozoic climates and plate motions inferred from major element chemistry of lutites. Nature 299, Pp. 715–717.

Nzeukou, N. A., Tsozué, D., Kagonbé, P. B., Balo, M. A., Fankam, D., Ngosi, S., Nkoumbou, C., Fagel, N. 2021. Clayey Soils from Boulgou (North Cameroon): Geotechnical, Mineralogical, Chemical Characteristics and Properties of Their Fired Products. SN Applied Sciences, 3, Article No.551. https://doi.org/10.1007/s42452-021-04541-4.

Okiotor, M.E., and Ighodaro, E.J. 2020. Geotechnical appraisal of the Mamu shales exposure around Igodor in the Benin flank of Anambra basin. Journal of Applied and Environmental Management, 24 (3), Pp. 489-493.

Olajubaje, T. A., Akande, S. O., Adeoye, J. A., Adekeye, O. A., Friedrich, C. 2018. Depositional Environments and Geochemical Assessments of the Bende Ameki Formation Potential as Petroleum Source Rocks in the Ogbunike Quarry, South-Eastern Nigeria Doi: 10.19044/esj.2018.v14n27p157 URL:http://dx.doi.org/10.19044/esj.2018.v14n27p157

Omoruyi D.I., Ilevbare M., Ehinlaiye A.C. Akujieze C.N. 2022. Geochemical Discriminant for provenance characterization of some clay Deposits in Edo state, Nigeria.

Omoruyi, D. I, Ilevbare, M., Ehinlaiye A. O., Akujieze, C. N., 2022. Geochemical Discriminant for Provenance Characterization of Some Clay Deposits in Edo State, Nigeria. International Journal of Earth Sciences Knowledge and Applications 4 (3) Pp. 407-418

Opara, K.D., Onyekuru, S.O., Iwuagwu, C.J., Opara, A.I., Echetama, H.N., Njoku, J.O., Onyeanwu, P.B., Nwachukwu, C.K., Anozie, H.C. and Manuemelula, E.U 2020. Sandstone and Pebble Facies in Okigwe Anduturu Axis Anambra Basin, Southeastern Nigeria: Constraints On Provenance and Tectonic Environment. International Journal of Advanced Academic Research. ISSN: 2488-9849 Vol. 7, Issue 10. www.ijaar.org

Oti, C. F. and Nwachukwu, A. E., 2021: Petrographic and geochemical evidence for provenace, paleoweathering and tectonic setting of the Maastrichtian-Paleocene sandstones from Anambra basin, southeast Nigeria. Journal of African Earth Sciences, 179, 104225. https://doi.org/10.1016/j.jafrearsci.2021.104225

Rakhimov, I.R., Saveliev, D.E., Rassomakhin, M.A., Samigullin, A.A. 2022. Chromian spinels from Kazanian-stage placers in the southern pre-urals, Bashkira, Russia: morphological and chemical features and evidence for provenance. Minerals 12 (7), Pp. 849.

Roser, B.P. 1996. Reconnaissance Sandstone Geochemistry, Provenance, and Tectonic Setting of the Lower Pleozoic Terrains of the West Coast and Nelson, New Zealand. New Zealand. Journal of Geology and Geophysics 39: Pp. 1-16.

Rui, Y., et al., 2019. Cryptic Footprints of Rare Earth Elements on Natural Resources and Living Organisms. Elsevier. Environmental International 785–800. https://doi.org/10.1016/j.envint.2019.03.022.

Saleh, G.M., Abdalla, H.M., Matsueda, H., Ishihara, S. 2023. Phanerozoic Rare Earth Elements Resources of Egypt: Metallogenetic and Mineral Exploration Constraints. The Phanerozoic Geology and Natural Resources of Egypt, Pp. 581-611.

Solomon, A., Christian, J. E., Rein, T. T., and Diego, M. B. 2021. Review of the Relationship between Aggregates Geology and Los Angeles and Micro-Deval tests. Bulletin of Engineering Geology and the Environment (2021) 80: Pp. 1963–1980 https://doi.org/10.1007/s10064-020-02097-y

Wronkiewicz, D.J. and Condie, K.C. 1987. Geochemistry of Archean Shales from the wit water strand super group, South Africa, source area weathering and provenance. Geochim. Cosmochim. Acta, 51, Pp. 2401-2416.

Zhang, S., Yang, T., Sun, X., Wei, H. and Wu, Y. 2021. Geochemical Characteristics and Provenance of the Upper Jurassic Linxi Formation in the Northeastern Junggar Basin, China: Implications for Paleoclimate and Paleogeography. Journal of Petroleum Science and Engineering, 202, 108596.